



Cite this: *Green Chem.*, 2025, **27**, 9452



Received 21st May 2025,

Accepted 14th July 2025

DOI: 10.1039/d5gc02521d

rsc.li/greenchem

## Renewable energy-driven synthesis of bioactive quinolinones through photocatalytic and electrochemical activation†

Qingge Zhao,<sup>a</sup> Mengyu Peng,<sup>a</sup> Huimin Li,<sup>a</sup> Longqiang Zhao,<sup>a</sup> Xinyue Song,<sup>a</sup> Peiyao Zhao,<sup>a</sup> Shoucai Wang,<sup>\*b</sup> Guangbin Jiang <sup>\*a</sup> and Fanghua Ji <sup>\*a</sup>

We present an innovative photocatalytic system for sustainable quinolin-2(1*H*)-one synthesis with broad substrate scope under mild, oxidant-free conditions, overcoming limitations of harsh traditional methods and high-pressure CO dependency. A complementary electrochemical strategy demonstrates analogous carbonylative cyclization as a proof-of-concept, while the sunlight-driven

protocol achieves exceptional versatility across diverse substrates, directly accessing pharmaceutically vital derivatives. This dual energy-activation paradigm (light/electricity) merges operational safety and environmental compatibility, establishing the photocatalytic route as a scalable platform for heterocycle construction while outlining electrochemical potential for future development.

### Green foundation

1. Our work centers on a green synthesis strategy that uses solar energy as a light source, eliminating the need for toxic oxidants. By employing readily available and inexpensive CO gas as the carbonyl source, we achieve high atom economy in the production of quinolinone.
2. Utilizing solar energy, we have overcome the conventional reliance on high-temperature and high-pressure CO, a significant limitation of traditional methods. This innovation reduces risks associated with extreme conditions and enhances both safety and sustainability.
3. Our future work will advance sustainable catalysis by utilizing CO<sub>2</sub> as a renewable carbonyl precursor and designing efficient earth-abundant metal catalysts, thereby elevating the methodology's environmental profile while maintaining its synthetic utility for pharmaceutical applications.

## Introduction

Sunlight, as a green, clean, and abundantly available renewable energy source, has long been a focal point in chemical research for its efficient utilization and conversion.<sup>1</sup> While visible light constitutes the predominant component of solar radiation, most organic molecules lack inherent visible-light absorption capacity, necessitating photocatalysts to mediate the transformation of photonic energy into chemical energy.<sup>2</sup> The potent redox capabilities

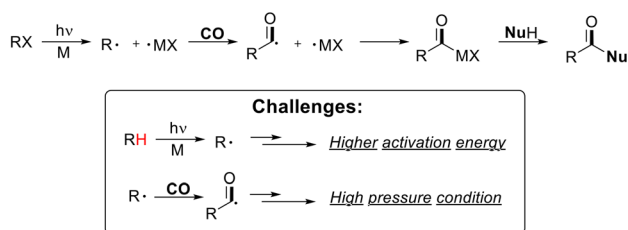
of photoexcited catalysts serve as the cornerstone for this energy conversion process.<sup>3</sup> Guided by green chemistry principles, advancements in visible-light photocatalysis have propelled novel synthetic methodologies, particularly in carbonylation reactions, offering innovative pathways for constructing carbonyl compounds.<sup>4</sup> Radical carbonylation reactions employing visible light as a green catalyst demonstrate superior efficiency, environmental compatibility, and selectivity compared to traditional carbonylative approaches.<sup>5</sup> These transformations typically proceed *via* oxidative quenching or reductive quenching pathways, both relying on acyl radical intermediates generated from precursors such as halides, pseudo-halides, or carboxylic acids.<sup>6</sup> Nevertheless, the direct generation of alkyl/aryl radicals from C–H precursors under photocatalytic conditions remains underexplored, primarily due to challenges in overcoming energy barriers for C–H bond activation. Moreover, the prevalent requirement for high-pressure CO gas as the carbonyl source poses safety concerns and operational inefficiencies, underscoring the need for ambient-pressure alternatives in acyl radical formation (Scheme 1).<sup>7</sup>

Visible-light photocatalysis and organic electrocatalysis employ photons and electrons as respective reagents, both

<sup>a</sup>Guangxi Key Laboratory of Electrochemical and Magnetochemical Function Materials, College of Chemistry and Bioengineering, Guilin University of Technology, 12 Jiangnan Road, Guilin 541004, China. E-mail: fanghua.ji@glut.edu.cn, jianggb@glut.edu.cn

<sup>b</sup>State Key Laboratory of Chemistry and Utilization of Carbon Based Energy Resources, Key Laboratory of Oil and Gas Fine Chemicals, Ministry of Education & Xinjiang Uygur Autonomous Region, Urumqi Key Laboratory of Green Catalysis and Synthesis Technology, College of Chemistry, Xinjiang University, Urumqi 830017, P. R. China. E-mail: 784331187@qq.com

† Electronic supplementary information (ESI) available. See DOI: <https://doi.org/10.1039/d5gc02521d>



**Scheme 1** Visible light-induced carbonylation by interplay of metal catalyst and carbon radicals.

generating reactive radical species or radical ions through single-electron transfer processes.<sup>8</sup> This mechanistic congruence enables successful translation of photochemically driven transformations into electrochemical regimes.<sup>9</sup> Building upon these fundamental principles, we have developed complementary solar-driven photocatalytic and electrochemical carbonylation-cyclization systems for constructing quinolin-2(1*H*)-one derivatives which are structurally versatile and biologically significant heterocycles.

Quinolinone scaffolds, recognized as ubiquitous structural motifs in pharmacologically privileged natural products and therapeutic agents, demonstrate broad-spectrum bioactivity with significant therapeutic relevance across multiple disease paradigms.<sup>10</sup> As illustrated in Fig. 1, representative derivatives including PARP-1 inhibitors, crinasiadine, MAPK inhibitors, and INOS modulators exhibit potent antitumor efficacy through malignant cell growth suppression, coupled with anti-inflammatory mechanisms, while HBV-targeting analogues function by specifically inhibiting viral replication machinery.<sup>11</sup> This structural versatility underscores the imperative for developing sustainable catalytic strategies enabling atom-economical construction of quinolinone architectures, which represents a critical endeavor in modern synthetic methodology.

Conventional synthetic approaches to quinolin-2(1*H*)-one derivatives frequently require harsh conditions (elevated temperatures, high pressures, and strong bases), suffer from prolonged reaction durations, and exhibit poor atom economy, underscoring the urgent need for greener and more efficient methodologies (Scheme 2a).<sup>12</sup> Building on our group's expertise in catalytic systems, we have devised a sunlight-driven

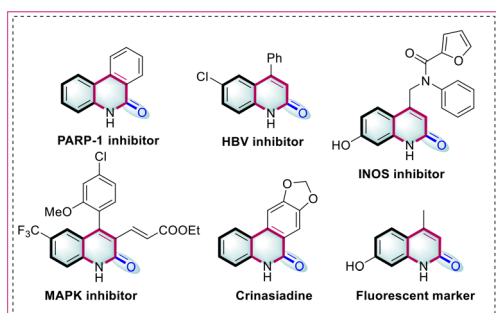
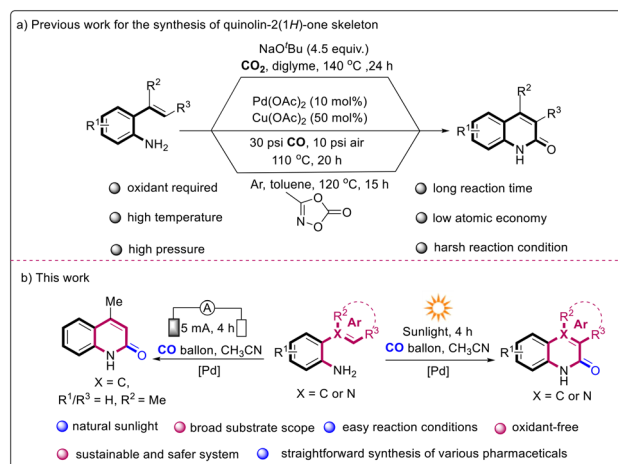


**Fig. 1** Selected quinolin-2(1*H*)-one-containing drugs.



**Scheme 2** Strategies for the synthesis of quinolin-2(1*H*)-ones.

photocatalytic carbonylative cyclization strategy that operates under mild conditions with broad substrate tolerance, eliminating the need for external oxidants and ensuring operational sustainability.<sup>13</sup> Notably, this transformation is equally achievable *via* an electrochemical catalytic strategy (Scheme 2b). Remarkably, the protocol has enabled efficient synthesis of pharmaceutically relevant derivatives, significantly elevating its practical applicability in medicinal chemistry.

## Results and discussion

We selected 2-(prop-1-en-2-yl)aniline **1a** as the model substrate under carbon monoxide atmosphere with sunlight irradiation for reaction optimization (Table 1). Systematic parameter

**Table 1** Optimization of the reaction conditions<sup>a</sup>

Entry	Deviation from standard conditions	Yield <sup>b</sup> (%)
1	<b>None</b>	<b>87</b>
2	Pd(PPh <sub>3</sub> ) <sub>4</sub> instead of Pd(OAc) <sub>2</sub>	54
3	Pd(PPh <sub>3</sub> ) <sub>2</sub> Cl <sub>2</sub> instead of Pd(OAc) <sub>2</sub>	0
4	TEAB instead of TBAB	85
5	NaCl instead of TBAB	32
6	THF instead of CH <sub>3</sub> CN	40
7	DMF instead of CH <sub>3</sub> CN	0
8	Without HOAc	73
9	TMA instead of HOAc	79
10	TFA instead of HOAc	0
11	Without Pd(OAc) <sub>2</sub>	0
12	Without TBAB	Trace
13	No light	Trace

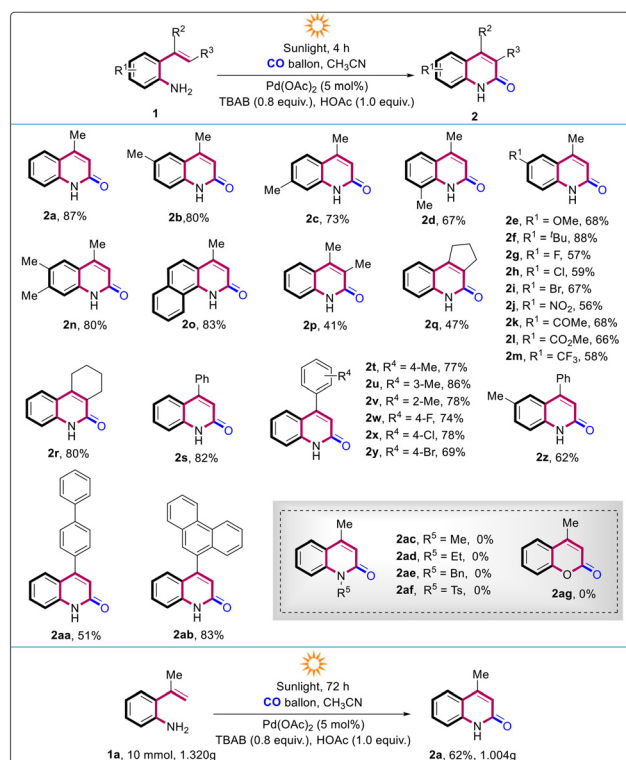
<sup>a</sup> Reaction conditions: **1a** (0.2 mmol), Pd(OAc)<sub>2</sub> (5 mol%), TBAB (0.16 mmol), HOAc (0.2 mmol), CH<sub>3</sub>CN (3 mL), CO balloon, sunlight irradiation for 4 h at room temperature. <sup>b</sup> Isolated yield.

screening identified optimal conditions as: 0.2 mmol of **1a** in MeCN with tetrabutylammonium bromide (TBAB) and HOAc as additives, achieving 87% isolated yield (entry 1). Catalyst evaluation revealed critical structural dependence: substituting the standard Pd(OAc)<sub>2</sub> catalyst with Pd(PPh<sub>3</sub>)<sub>4</sub> reduced the yield to 54%, while Pd(PPh<sub>3</sub>)<sub>2</sub>Cl<sub>2</sub> completely inhibited product formation (entries 2 and 3). The additive screening process clearly highlighted the superior performance of TBAB. When TBAB was substituted with tetraethylammonium bromide (TEAB), the yield experienced only a marginal decline to 85%. In contrast, the use of NaCl led to a substantial reduction in yield, plummeting to just 32% (entries 4 and 5). After screening various solvents, acetonitrile was identified as the optimal choice for this reaction (entries 6 and 7). Acid optimization confirmed HOAc's necessity: neutral conditions gave 73% yield (entry 8), with trimethylacetic acid (TMA) and trifluoroacetic acid (TFA) performing suboptimally (entries 9 and 10). Complete reaction inhibition occurred without Pd(OAc)<sub>2</sub>, confirming the catalyst's irreplaceability (entry 11). TBAB removal reduced yield to 15%, indicating its critical yet non-absolute role in ion pairing (entry 12). Photon deprivation resulted in trace product, demonstrating sunlight's essential activation energy (entry 13).

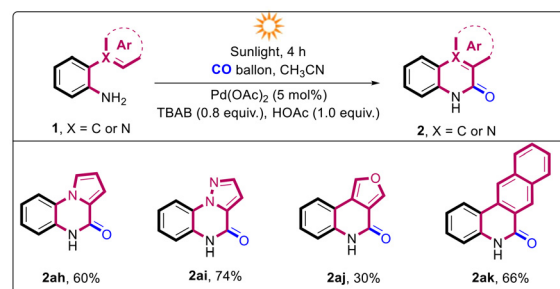
With optimized conditions established, we systematically evaluated the methodology's scope and limitations (Scheme 3). Initial positional variation of benzene ring substituents

(**2b–2d**) demonstrated consistent efficiency across all substitution patterns. Electronic perturbation studies revealed broad tolerance for both electron-donating (methoxy, *tert*-butyl) and electron-withdrawing groups (halogen, trifluoromethyl, nitro), achieving excellent yields (**2e–2m**), while sterically demanding 3,5-dimethyl (**2n**) and vinyl-naphthylamine (**2o**) derivatives maintained high reactivity. Investigation of *o*-alkenyl substitutions showed diminished yields for bis(methyl)-(**2p**, 41%) and cyclopentyl-substituted (**2q**, 47%) systems, contrasting sharply with the cyclohexenyl analogue **2r** (80%), where enhanced efficiency likely arises from the fused polycyclic system's superior stability. Targeting pharmacologically relevant 4-aryl-2-quinolinones, *ortho*  $\alpha$ -styrenyl anilines (**2s–2z**) delivered moderate-to-excellent yields (62–86%), with extended  $\pi$ -systems (biphenyl **2aa**, phenanthrene **2ab**) confirming structural versatility. Critical limitations emerged: *N*-substituted anilines failed to react, and phenolic analogues proved inactive. We propose that this phenomenon can be attributed to the presence of a substituent on the nitrogen atom. We propose that the presence of substituents on the substrate amine may hinder the subsequent coordination with palladium and the insertion of the carbonyl group. Similarly, phenolic analogs seem to be unreactive due to their structural limitations. Practical utility was demonstrated through gram-scale synthesis (10.0 mmol of **1a**), affording product in 62% yield.

Encouraged by the successful application of *ortho*-alkenyl anilines and drawing mechanistic parallels with established sp<sup>2</sup> C–H activation pathways, we systematically extended the carbonylation protocol to *o*-aryl anilines bearing diverse heterocycles (Scheme 4). While pyrrole- (**2ah**, 60%) and naphthalene-containing (**2ak**, 66%) substrates demonstrated moderate reactivity, pyrazole analogues (**2ai**, 74%) exhibited enhanced efficiency, likely benefiting from nitrogen's dual coordination capability. Notably, the oxygen-rich furan system (**2aj**, 30%) displayed significantly reduced yield, potentially due to competing oxygen coordination or electronic deactivation. This marked variation (30–74%) highlights the critical influence of heteroatom identity and electronic environment on catalytic performance. Nevertheless, successful transformation of these



**Scheme 3** Substrate scope of 2-alkenylanilines. Reaction conditions: **1** (0.2 mmol), Pd(OAc)<sub>2</sub> (5 mol%), TBAB (0.16 mmol), HOAc (0.2 mmol), CH<sub>3</sub>CN (3 mL), CO balloon, sunlight irradiation for 4 h at room temperature. Isolated yield.

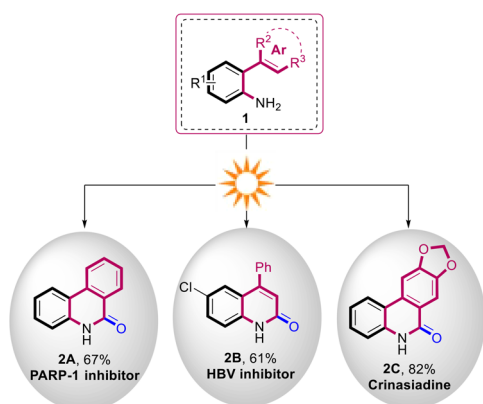


**Scheme 4** Scope of 2-heteroaryl anilines. Reaction conditions: **1** (0.2 mmol), Pd(OAc)<sub>2</sub> (5 mol%), TBAB (0.16 mmol), HOAc (0.2 mmol), CH<sub>3</sub>CN (3 mL), CO balloon, sunlight irradiation for 4 h at room temperature. Isolated yield.

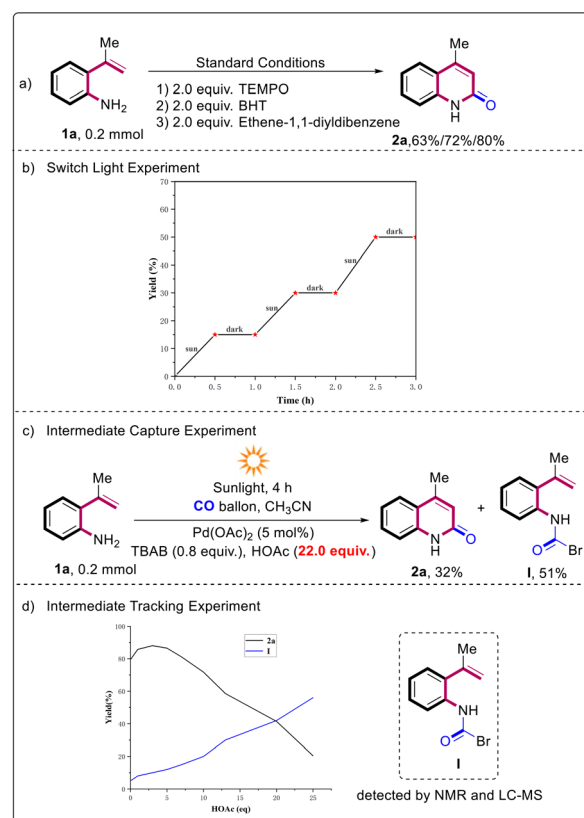
structurally distinct systems-spanning electron-rich five-membered heterocycles (pyrrole, furan) to extended  $\pi$ -systems (naphthalene)-confirms the method's adaptability to diverse aromatic architectures, while establishing clear boundaries for optimal heteroatom selection in carbonylative cyclization processes.

Significantly, this methodology demonstrates robust applicability in constructing structurally complex quinolinones with established bioactivity, effectively extending to pharmacologically valuable targets including PARP-1 inhibitor phenanthridin-6(5*H*)-one **2A**, hepatitis B virus suppressor 6-chloro-4-phenylquinolin-2(1*H*)-one **2B**, and the naturally inspired alkaloid [1,3]dioxolo[4,5-*j*]phenanthridin-6(5*H*)-one **2C** (crinasidine) (Scheme 5). The successful implementation of these syntheses underscores the platform's capacity to access diverse bioactive architectures through streamlined carbonylative cyclization, positioning it as a strategic tool for modular assembly of drug-like heterocycles. This multifaceted adaptability not only confirms the method's proficiency in accessing pharmaceutically privileged molecular architectures but also underscores its strategic value in streamlining lead candidate evolution within medicinal chemistry campaigns.

To elucidate the reaction mechanism, systematic control experiments were conducted. Radical pathway interrogation *via* TEMPO, BHT, and ethene-1,1-diylidibenzene scavengers revealed no significant inhibition, effectively excluding radical intermediates (Scheme 6a). Photochemical necessity was further established through light interruption experiments, with the complete reaction arrest under dark conditions unequivocally confirming the continuous photon requirement and providing mechanistic evidence for photoinduced catalytic cycle initiation (Scheme 6b). Mechanistic probing through acetic acid loading variation identified optimal performance at three equivalents, with excessive acid (22 equivalents) redirecting the pathway toward byproduct **I** formation (Scheme 6c–d). This acid-dependent behavior suggests proton concentration modulates reaction trajectory: moderate  $H^+$  levels facilitate cat-



**Scheme 5** Synthetic utilization. Reaction conditions: **1** (0.2 mmol), Pd(OAc)<sub>2</sub> (5 mol%), TBAB (0.16 mmol), HOAc (0.2 mmol), CH<sub>3</sub>CN (3 mL), CO balloon, sunlight irradiation for 4 h at room temperature. Isolated yield.

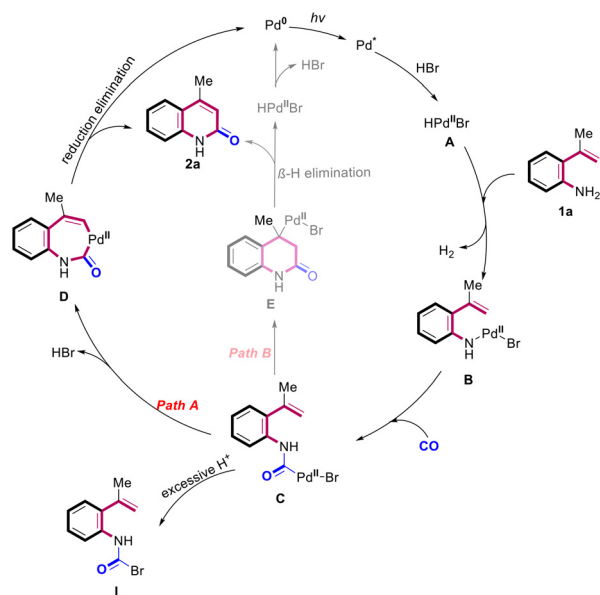


**Scheme 6** Control experiments.

alysis, whereas excess protons impede olefinic C–H activation, favoring uncyclized byproduct **I**. These collective insights critically inform the proposed mechanistic framework.

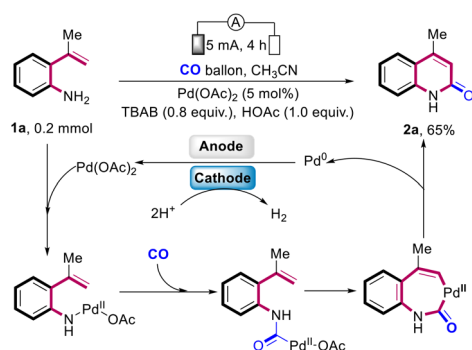
The proposed mechanism commences with photoexcitation of Pd<sup>0</sup> to its reactive state, followed by oxidative addition of hydrogen bromide to form a palladium hydride complex.<sup>14</sup> Subsequent coordination of substrate **1a** induces hydrogen liberation while generating intermediate **B**, which undergoes CO insertion into the Pd–N bond to yield intermediate **C**. Divergent elimination pathways were identified: Pathway A proceeds *via* C–H activation of intermediate **C**, ejecting HBr to form a seven-membered palladacycle **D** that releases product **2a** through reductive elimination, regenerating Pd<sup>0</sup>. Alternatively, Pathway B involves vinyl insertion of the Pd–CO moiety to create alkylpalladium species **E**, where  $\beta$ -hydroelimination furnishes **2a** alongside Pd<sup>0</sup> recovery. Proton saturation effects were mechanistically rationalized, wherein elevated  $H^+$  concentrations obstruct olefinic C–H cleavage in intermediate **C**, diverting the pathway toward uncyclized byproduct **I** formation. Critically, the light-dependent activation steps observed in light interruption experiments strongly favor Pathway A as the predominant mechanism (Scheme 7).

Photocatalytic and electrochemical systems exhibit fundamental mechanistic parallels, with visible light-mediated processes employing photons and organic electrosynthesis utilizing electrons as respective reagents, both initiating transform-



**Scheme 7** Possible reaction mechanism under photocatalytic conditions.

ations through single-electron transfer to generate reactive radical intermediates.<sup>15</sup> This shared activation paradigm enables transference of chemical transformations between photochemical and electrochemical regimes, as evidenced by our successful implementation of carbonylative cyclization under purely electrochemical conditions. Mechanistic interrogation reveals a catalytic cycle commencing with nucleophilic attack of the aniline nitrogen on Pd<sup>II</sup>, forging a Pd–N bond with concomitant acetic acid liberation (Scheme 8). Subsequent CO insertion into the Pd–N linkage yields a Pd-carbamoyl Intermediate, whose C–H activation generates a seven-membered palladacycle that releases product **2a** via reductive elimination while regenerating Pd<sup>0</sup>. Anodic reoxidation of Pd<sup>0</sup> to Pd<sup>II</sup> sustains catalytic continuity, while concurrent cathodic proton reduction to H<sub>2</sub> maintains charge equilibrium throughout the electrochemical cycle.



**Scheme 8** Possible reaction mechanism under electrocatalytic conditions.<sup>a, b</sup> <sup>a</sup> Reaction conditions: **1a** (0.2 mmol), Pd(OAc)<sub>2</sub> (5 mol%), TBAB (0.8 equiv.), HOAc (1.0 equiv.), CH<sub>3</sub>CN (3 mL) in an undivided cell with a graphite cloth anode, a nickel foam cathode, CO balloon, rt, 5 mA, 4 h. <sup>b</sup> Isolated yield.

## Conclusions

In summary, this work demonstrates the viability of energy-mediated catalytic systems for sustainable heterocycle synthesis, where sunlight-driven photocatalysis emerges as a robust platform for constructing quinolin-2(1*H*)-ones with operational simplicity, broad functional group tolerance, and direct access to bioactive derivatives. By establishing a dual activation paradigm (photonic/electronic), we reconcile synthetic efficiency with green chemistry principles—eliminating harsh reagents, minimizing hazardous waste, and circumventing high-pressure CO requirements. While the photocatalytic route showcases immediate applicability in drug-relevant molecule production, the complementary electrochemical approach lays groundwork for future energy-adaptive synthetic designs. Collectively, this research redefines heterocyclic architecture assembly through renewable energy utilization, prioritizing atom economy and scalability while expanding the toolbox for medicinal chemistry innovation.

## Author contributions

Fanghua Ji, Guangbin Jiang, Shoucai Wang conceived the study; Qingge Zhao performed the experiments, and prepared the ESI,<sup>†</sup> Mengyu Peng, Huimin Li, Longqiang Zhao made some of the substrates.

## Conflicts of interest

There are no conflicts to declare.

## Data availability

The authors confirm that the data supporting the findings of this study are available within the article and its ESI.<sup>†</sup>

The original data that support the findings of this study are available from the corresponding author, upon reasonable request.

## Acknowledgements

This work was supported by the Nature Science Foundation of China (22401057 and 22461014), Guangxi Natural Science Foundation (2020GXNSFAA297227), and Key Laboratory of Electrochemical and Magnetochemical Function Materials (EMFM20241103).

## References

- (a) H. Tan, H. Li, W. Ji and L. Wang, *Angew. Chem., Int. Ed.*, 2015, **54**, 8374–8377; (b) J.-D. Guo, X.-L. Yang, B. Chen, C.-H. Tung and L.-Z. Wu, *Green Chem.*, 2021, **23**, 7193–

- 7198; (c) C.-J. Wu, X.-Y. Li, T.-R. Li, M.-Z. Shao, L.-J. Niu, X.-F. Lu, J.-L. Kan, Y. Geng and Y.-B. Dong, *J. Am. Chem. Soc.*, 2022, **144**, 18750–18755; (d) J. Xie, S. Shi, T. Zhang, N. Mehrkens, M. Rudolph and A. S. K. Hashmi, *Angew. Chem., Int. Ed.*, 2015, **54**, 6046–6050; (e) A. Rana, B. K. Malviya, D. K. Jaiswal, P. Srihari and A. K. Singh, *Green Chem.*, 2022, **24**, 4794–4799.
- 2 (a) K. Kwon, R. T. Simons, M. Nandakumar and J. L. Roizen, *Chem. Rev.*, 2022, **122**, 2353–2428; (b) W.-M. Cheng and R. Shang, *ACS Catal.*, 2020, **10**, 9170–9196; (c) K. P. S. Cheung, S. Sarkar and V. Gevorgyan, *Chem. Rev.*, 2022, **122**, 1543–1625.
- 3 (a) X. Tong, Z. Wu, H. T. Ang, Y. Miao, Y. Lu and J. Wu, *ACS Catal.*, 2024, **14**, 9283–9293; (b) H. Li, K.-C. Yu, J.-K. Su, W. Ouyang, N.-L. Fan and X.-G. Hu, *Green Chem.*, 2022, **24**, 8280–8291; (c) Y. Lei, J. Yang, Y. Wang, H. Wang, Y. Zhan, X. Jiang and Z. Xu, *Green Chem.*, 2020, **22**, 4878–4883; (d) I. Quirós, M. Martín, M. Gomez-Mendoza, M. J. Cabrera-Afonso, M. Liras, I. Fernández, L. Nóvoa and M. Tortosa, *Angew. Chem., Int. Ed.*, 2024, **63**, e202317683; (e) Y. Moon, B. Park, I. Kim, G. Kang, S. Shin, D. Kang, M.-H. Baik and S. Hong, *Nat. Commun.*, 2019, **10**, 4117–4125; (f) M.-M. Lu, N. Deng, S.-Y. Li, R.-J. Tong, J. Xu and H.-J. Xu, *Green Chem.*, 2024, **26**, 8694–8700; (g) N. Kim, C. Lee, T. Kim and S. Hong, *Org. Lett.*, 2019, **21**, 9719–9723; (h) W.-J. Zhou, Z.-H. Wang, L.-L. Liao, Y.-X. Jiang, K.-G. Cao, T. Ju, Y. Li, G.-M. Cao and D.-G. Yu, *Nat. Commun.*, 2020, **11**, 3263–3271.
- 4 (a) Z. Zhang, J.-H. Ye, T. Ju, L.-L. Liao, H. Huang, Y.-Y. Gui, W.-J. Zhou and D.-G. Yu, *ACS Catal.*, 2020, **10**, 10871–10885; (b) X.-Q. Hu, Z.-K. Liu and W.-J. Xiao, *Catalysts*, 2020, **10**, 1054–1079.
- 5 (a) X.-B. Yan, N. Wang, J. Zhou, H. Ge, Z. Wang, Y. Lin and H. Shui, *Org. Lett.*, 2024, **26**, 6518–6522; (b) B. Lu, Z. Zhang, M. Jiang, D. Liang, Z. He, F. Bao, W. Xiao and J. Chen, *Angew. Chem., Int. Ed.*, 2023, **62**, e202309460; (c) P. Tung and N. P. Mankad, *J. Am. Chem. Soc.*, 2023, **145**, 9423–9427; (d) J. Zhang, L.-C. Wang, Y. Wang and X.-F. Wu, *Green Chem.*, 2024, **26**, 11686–11694.
- 6 (a) M. Hosseini-Sarvari and Z. Akrami, *Catal. Sci. Technol.*, 2021, **11**, 956–969; (b) N. Micic and A. Polyzos, *Org. Lett.*, 2018, **20**, 4663–4666; (c) J.-B. Peng, X. Qi and X.-F. Wu, *ChemSusChem*, 2016, **9**, 2279–2283; (d) Q.-Q. Zhou, W. Guo, W. Ding, X. Wu, X. Chen, L.-Q. Lu and W.-J. Xiao, *Angew. Chem., Int. Ed.*, 2015, **54**, 11196–11199; (e) A. Cartier, E. Levernier, A.-L. Dhimane, T. Fukuyama, C. Ollivier, I. Ryu and L. Fensterbank, *Adv. Synth. Catal.*, 2020, **362**, 2254–2259.
- 7 (a) T. Kawamoto, A. Sato and I. Ryu, *Chem. – Eur. J.*, 2015, **21**, 14764–14767; (b) S. Sumino, A. Fusano, T. Fukuyama and I. Ryu, *Acc. Chem. Res.*, 2014, **47**, 1563–1574; (c) S. Sumino, T. Ui, Y. Hamada, T. Fukuyama and I. Ryu, *Org. Lett.*, 2015, **17**, 4952–4955; (d) B. Lu, M. Xu, X. Qi, M. Jiang, W.-J. Xiao and J.-R. Chen, *J. Am. Chem. Soc.*, 2022, **144**, 14923–14935; (e) Y. Zhang, Y. Yuan, H.-Q. Geng, J.-X. Xu and X.-F. Wu, *J. Catal.*, 2022, **413**, 214–220; (f) M.-L. Yang and X.-F. Wu, *Green Chem.*, 2025, **27**, 5257–5264.
- 8 (a) W.-J. Wei, Y.-Q. Zeng, X.-F. Liang, F.-H. Cui, M.-R. Wang, Y.-M. Pan, W.-G. Duan and H.-T. Tang, *Green Chem.*, 2025, **27**, 1006–1012; (b) Y. Wang, S. Dana, H. Long, Y. Xu, Y. Li, N. Kaplaneris and L. Ackermann, *Chem. Rev.*, 2023, **123**, 11269–11335; (c) S. R. Waldvogel, S. Lips, M. Selt, B. Riehl and C. J. Kampf, *Chem. Rev.*, 2018, **118**, 6706–6765; (d) P. R. D. Murray, J. H. Cox, N. D. Chiappini, C. B. Roos, E. A. McLoughlin, B. G. Hejna, S. T. Nguyen, H. H. Ripberger, J. M. Ganley, E. Tsui, N. Y. Shin, B. Koronkiewicz, G. Qiu and R. R. Knowles, *Chem. Rev.*, 2022, **122**, 2017–2291.
- 9 (a) Y. Zhang, Z. Lin and L. Ackermann, *Chem. – Eur. J.*, 2021, **27**, 242–246; (b) Y. Zhao, Y.-L. Lai, K.-S. Du, D.-Z. Lin and J.-M. Huang, *J. Org. Chem.*, 2017, **82**, 9655–9661; (c) A. N. Dinh, A. D. Nguyen, E. M. Aceves, S. T. Albright, M. R. Cedano, D. K. Smith and J. L. Gustafson, *Synlett*, 2019, 1648–1655; (d) X.-Y. Qian, S.-Q. Li, J. Song and H.-C. Xu, *ACS Catal.*, 2017, **7**, 2730–2734; (e) S. Cai, Y. Xu, D. Chen, L. Li, Q. Chen, M. Huang and W. Weng, *Org. Lett.*, 2016, **18**, 2990–2993; (f) K. Tong, X. Liu, Y. Zhang and S. Yu, *Chem. – Eur. J.*, 2016, **22**, 15669–15673.
- 10 (a) H. L. Schmitt, D. Martymianov, O. Green, T. Delcaillau, Y. S. Park Kim and B. Morandi, *J. Am. Chem. Soc.*, 2024, **146**, 4301–4308; (b) L. B. Rao, C. Sreenivasulu, D. R. Kishore and G. Satyanarayana, *Tetrahedron*, 2022, **127**, 133093; (c) X.-M. Chu, C. Wang, W. Liu, L.-L. Liang, K.-K. Gong, C.-Y. Zhao and K.-L. Sun, *Eur. J. Med. Chem.*, 2019, **161**, 101–117; (d) E. A. Larsson, A. Jansson, F. M. Ng, S. W. Then, R. Panicker, B. Liu, K. Sangthongpitag, V. Pendharkar, S. J. Tai, J. Hill, C. Dan, S. Y. Ho, W. W. Cheong, A. Poulsen, S. Blanchard, G. R. Lin, J. Alam, T. H. Keller and P. Nordlund, *J. Med. Chem.*, 2013, **56**, 4497–4508; (e) Y. Li and L. L. Wong, *Angew. Chem., Int. Ed.*, 2019, **58**, 9551–9555; (f) X. Yu, S. Yang, N. Yan, Y. Fu, Y. Li, W. Wang and M. Bao, *Green Chem.*, 2024, **26**, 10818–10823.
- 11 (a) Z. Jin, *Nat. Prod. Rep.*, 2009, **26**, 363; (b) Y.-D. Shao, M.-M. Dong, Y.-A. Wang, P.-M. Cheng, T. Wang and D.-J. Cheng, *Org. Lett.*, 2019, **21**, 4831–4836; (c) T. Haikarainen, M. Narwal, P. Joensuu and L. Lehtiö, *ACS Med. Chem. Lett.*, 2014, **5**, 18–22; (d) C. Hu, L. Wang, X. Yang, Y. Fu and Z. Du, *Org. Lett.*, 2024, **26**, 7783–7788; (e) S. E. Nasrabad, A. Kuzhandaivel, M. Mladinic and A. Nistri, *Cell. Mol. Neurobiol.*, 2011, **31**, 503–508; (f) R. Labaudiniere, W. Hendel, B. Terlain, F. Cavy, O. Marquis and N. Dereu, *J. Med. Chem.*, 1992, **35**, 4306–4314; (g) P. Cheng, Q. Zhang, Y.-B. Ma, Z.-Y. Jiang, X.-M. Zhang, F.-X. Zhang and J.-J. Chen, *Bioorg. Med. Chem. Lett.*, 2008, **18**, 3787–3789; (h) P. R. Angibaud, M. G. Venet, W. Filliers, R. Broeckx, Y. A. Ligny, P. Muller, V. S. Poncelet and D. W. End, *Eur. J. Org. Chem.*, 2004, 479–486.
- 12 (a) J. Nan, P. Chen, X. Gong, Y. Hu, Q. Ma, B. Wang and Y. Ma, *Org. Lett.*, 2021, **23**, 3761–3766; (b) Z. Zhang, L. Liao, S. Yan, L. Wang, Y. He, J. Ye, J. Li, Y. Zhi and D. Yu, *Angew. Chem., Int. Ed.*, 2016, **55**, 7068–7072; (c) J. Ferguson,

- F. Zeng, N. Alwis and H. Alper, *Org. Lett.*, 2013, **15**, 1998–2001.
- 13 (a) C. Kang, M. Li, W. Huang, S. Wang, M. Peng, L. Zhao, G. Jiang and F. Ji, *Green Chem.*, 2023, **25**, 8838–8844; (b) M. Peng, M. Li, L. Zhao, W. Huang, S. Wang, K. Chen, G. Jiang and F. Ji, *Org. Chem. Front.*, 2023, **10**, 5680–5684; (c) S. Wang, Z. Chen, F. Xue, Y. Zhang, B. Wang, S. Wu, Y. Xia, X. Zhao, G. Jiang, F. Ji and C. Liu, *Org. Chem. Front.*, 2024, **11**, 6019–6025; (d) M. Li, M. Peng, W. Huang, L. Zhao, S. Wang, C. Kang, G. Jiang and F. Ji, *Org. Lett.*, 2023, **25**, 7529–7534.
- 14 (a) P. Chuentragool, D. Kurandina and V. Gevorgyan, *Angew. Chem., Int. Ed.*, 2019, **58**, 11586–11598; (b) R. Shi, L. Lu, H. Xie, J. Yan, T. Xu, H. Zhang, X. Qi, Y. Lan and A. Lei, *Chem. Commun.*, 2016, **52**, 13307–13310; (c) W. Li, C. Liu, H. Zhang, K. Ye, G. Zhang, W. Zhang, Z. Duan, S. You and A. Lei, *Angew. Chem., Int. Ed.*, 2014, **53**, 2443–2446; (d) L. Niu, H. Yi, S. Wang, T. Liu, J. Liu and A. Lei, *Nat. Commun.*, 2017, **8**, 14226–14232.
- 15 (a) Y. Wu, L. Zeng, H. Li, Y. Cao, J. Hu, M. Xu, R. Shi, H. Yi and A. Lei, *J. Am. Chem. Soc.*, 2021, **143**, 12460–12466; (b) L. Zeng, H. Li, S. Tang, X. Gao, Y. Deng, G. Zhang, C.-W. Pao, J.-L. Chen, J.-F. Lee and A. Lei, *ACS Catal.*, 2018, **8**, 5448–5453; (c) H. Li, J. Peng, L. Zeng, L. Zhou, M. Shabbir, F. Xiao, J. Yuan, H. Yi and A. Lei, *Green Chem.*, 2024, **26**, 11177–11181.